

PREPARED FOR SUBMISSION TO JCAP

Anisotropic CMB distortions from non-Gaussian isocurvature perturbations

Atsuhisa Ota,^a Toyokazu Sekiguchi,^b Yuichiro Tada^{c,d} and Shuichiro Yokoyama^e

^aDepartment of Physics, Tokyo Institute of Technology,
Tokyo 152-8551, Japan

^bUniversity of Helsinki and Helsinki Institute of Physics,
P.O. Box 64, Helsinki 00014, Finland

^cKavli Institute for the Physics and Mathematics of the Universe (WPI), The University of Tokyo,
Kashiwa, Chiba 277-8583, Japan

^dDepartment of Physics, the University of Tokyo,
Bunkyo-ku 113-0033, Japan

^eDepartment of Physics, Rikkyo University,
3-34-1 Nishi-Ikebukuro, Toshima, Tokyo 223-8521, Japan

E-mail: a.ota@th.phys.titech.ac.jp, toyokazu.sekiguchi@helsinki.fi,
yuichiro.tada@ipmu.jp, shuichiro@rikkyo.ac.jp

Abstract. We calculate the CMB μ -distortion and the angular power spectrum of its cross-correlation with the temperature anisotropy in the presence of the non-Gaussian neutrino isocurvature density (NID) mode. While the pure Gaussian NID perturbations give merely subdominant contribution to $\langle\mu\rangle$ and vanishing $\langle\mu T\rangle$, the latter quantity can be large enough to be detected in the future when the NID perturbations $\mathcal{S}(\mathbf{x})$ are proportional to the square of a Gaussian field $g(\mathbf{x})$, i.e. $\mathcal{S}(\mathbf{x}) \propto g^2(\mathbf{x})$. In particular, large $\langle\mu T\rangle$ can be realized since Gaussian-squared perturbations can yield a relatively large bispectrum, satisfying the constraints from the power spectrum of CMB anisotropies, i.e. $\mathcal{P}_{SS}(k_0) \sim \mathcal{P}_g^2(k_0) \lesssim 10^{-10}$ at $k_0 = 0.05 \text{ Mpc}^{-1}$. We also forecast constraints from the CMB temperature and E-mode polarisation bispectra, and show that $\mathcal{P}_g(k_0) \lesssim 10^{-5}$ would be allowed from Planck data. We find that $\langle\mu\rangle$ and $|l(l+1)C_l^{\mu T}|$ can respectively be as large as 10^{-9} and 10^{-14} with uncorrelated scale-invariant NID perturbations for $\mathcal{P}_g(k_0) = 10^{-5}$. When the spectrum of the Gaussian field is blue-tilted (with spectral index $n_g \simeq 1.5$), $\langle\mu T\rangle$ can be enhanced by an order of magnitude.

Keywords: CMB distortion, non-Gaussianity, isocurvature perturbations

Contents

1	Introduction	1
2	Gaussian-squared type isocurvature perturbations	2
3	CMB μ-distortion	7
3.1	Homogeneous distortions	7
3.2	Inhomogeneous distortions	9
4	μT angular cross-correlation	10
5	Conclusions	13
A	Constraints from CMB angular bispectrum	14

1 Introduction

Inflationary scenario is a successful prescription to solve the initial condition problems of the hot Big Bang universe, and to determine the concrete theoretical model is one of the most important theme of recent observational cosmology [1]. Such an accelerated expanding universe predicts generation of the almost scale-invariant and Gaussian primordial fluctuations, which are well confirmed by a variety of cosmological observations including anisotropies in the Cosmic Microwave Background (CMB). The next step for further refinement may be to investigate deviations from Gaussian statistics, that is, to find non-Gaussianity [2]. The newest space mission Planck revealed that the non-linearity parameter $f_{\text{NL}} \lesssim \mathcal{O}(1)$, and many inflationary models are ruled out [3]. However, we should note that the CMB anisotropies are observables on relatively larger scale up to the multipole $l \sim 10^4$, and several orders of improvement of the resolution can be far beyond our current technology as well.

CMB spectrum distortions are alternative probes of the inflationary universe, for the distortions are created from small-scale density perturbations, without introducing new physics. Use of CMB distortions in conjunction with the CMB anisotropies on large scales may complementarily allow us to test the nature of primordial perturbations over many orders of scales. The distortions are basically classified into two types, y -type and μ -type,¹ depending on whether the system is thermal or not [6, 7]. Although thermalization of the photon system is efficient in the early universe, once the Compton scattering becomes ineffective around the redshift $z \sim 10^5$, deviations from the thermal equilibrium can no longer vanish since the Thomson scattering never transfers the photon energy through non-relativistic electrons. Then the distortion is parameterized as a non-thermal deviation from Planck distribution and we call it y -distortion. Another one is μ -distortion, which is a chemical potential in the Bose-Einstein distribution function of thermal photon system. Such a thermal deviation from Planck distribution is a consequence of re-thermalization under number conserving process such as the Compton scattering, so we can investigate the Compton dominant era around $z \sim 10^6$ [4, 5, 8–12]. Here we would focus only on this type of distortions.

¹ Some people discuss the intermediate type distortions [4, 5].

Typical magnitude of the μ -distortion which originates from the primordial curvature perturbations is 10^{-8} [10, 13–15] and the contributions from primordial tensor perturbations are subdominant [16, 17]. Constraints on these parameters are given by COBE FIRAS as $\mu < 9 \times 10^{-5}$ and $y < 1.5 \times 10^{-5}$ (95% C.L.) [18–20], and future space mission such as PIXIE [21] and PRISM [22] have potential to improve the constraints up to the order of 10^{-8} to 10^{-9} . Therefore, such distortions can be powerful tools to study primordial fluctuations.

Recently μT cross-correlation is also proposed as a probe of primordial non-Gaussianities down to small-scales [23, 24]. Roughly speaking, μ is proportional to the square of dimensionless temperature perturbations and then, the cross-correlation originates from the primordial three-point function. For the local type non-Gaussianity, the constraints on the non-linear parameter by PIXIE’s sensitivity are estimated as $f_{\text{NL}}^{\text{loc}} \lesssim 10^3$ in Ref. [23]. In this paper we calculate the μT cross-correlation in the presence of not only adiabatic but also isocurvature modes. The isocurvature modes do not necessarily follow the Gaussian distribution unlike the adiabatic modes and then they can cause large μT signals. Accordingly, we calculate contribution from Gaussian-squared isocurvature perturbations to the total cross-correlation as an example of the non-Gaussian case. Here we focus on the neutrino isocurvature density (NID) mode, which is not suppressed on small scales compared to adiabatic perturbations, in contrast to the matter isocurvature perturbations [25, 26]. We organize this paper as follows. In section 2, we present the formalisms of the power spectrum and bispectrum of the non-Gaussian isocurvature perturbations, with particular focus on the Gaussian-squared ones. Sections 3 and 4 show the calculations for μ and μT cross-correlations, respectively. We summarize the discussions and conclude in the final section. In appendix A, we comment on the constraints from CMB angular bispectrum.

2 Gaussian-squared type isocurvature perturbations

Models of generating the NID mode have been proposed in the literature [32–34]. So far, most of the models can be categorised into two types.² In one type, there assumed to be a large lepton asymmetry ($n_L/n_\gamma = \mathcal{O}(0.01) \gg n_B/n_\gamma = \mathcal{O}(10^{-9})$) in the universe. If fields sourcing the lepton asymmetry spatially fluctuate differently from inflaton (or in general fields reheating the universe), isocurvature perturbations inevitably arise between neutrino and the photon. In the other type, there assumed to exist dark radiation in the universe other than neutrino. In the context of structure formation, there is no distinction between dark radiation and neutrino, and they in effect consist a single fluid of neutrino species. Therefore, the NID mode is sourced if dark radiation is produced from fields which have isocurvature perturbations.

The NID mode can be non-Gaussian when so are source fields in themselves. In addition, even when the source fields are Gaussian, the so-called local-type non-Gaussianity in the NID mode can be induced in the similar fashion as in e.g. the curvaton and the modulated reheating models. In Ref. [35], several concrete models generating the local-type non-Gaussian

² In general, there should also be induced isocurvature perturbations between matter and radiation, depending on the details of production mechanisms (e.g. thermal or non-thermal ones) of baryon and CDM. However, as we mentioned in Introduction, when we focus on signatures in the CMB μ -distortion from isocurvature perturbations, contribution from matter isocurvature perturbations should be smaller than that from NID ones [25, 26]. Therefore for simplicity we omit the matter isocurvature perturbations throughout this paper, although there is a possibility that presence of them can somewhat change the bounds on non-Gaussian curvature and NID perturbations from the CMB bispectrum presented in Appendix A.

NID mode are discussed. A model of the type with dark radiation can be realised by generalising the curvaton model. When a curvaton field which creates non-Gaussian curvature perturbations decays into dark radiation with some branching ratio, non-Gaussian NID perturbations should also be created. On the other hand, a model of the type with large lepton asymmetry can be realised in the Affleck-Dine baryogenesis [36] with Q-ball formation [37]. In this case, the non-linear dependence of the amount of the lepton asymmetry on the initial value of the Affleck-Dine field leads to non-Gaussianity in the NID mode. Generation of non-Gaussian NID perturbations in the modulated reheating scenario can also be realized [34]. In this paper, we in particular focus on non-Gaussian isocurvature perturbations which are proportional to the square of Gaussian field (See (2.1)-(2.2)).³ Such the Gaussian-squared perturbations can be realized in the *ungaussiton* model [38–40].

Let us consider two fields \mathcal{R}_G and g both of which obey Gaussian statistics. In the above model, the curvature \mathcal{R} and the residual isocurvature perturbation \mathcal{S} can be written as

$$\mathcal{R}(\mathbf{x}) = \mathcal{R}_G(\mathbf{x}) + \gamma_1(g^2(\mathbf{x}) - \langle g^2 \rangle), \quad (2.1)$$

$$\mathcal{S}(\mathbf{x}) = \gamma_2(g^2(\mathbf{x}) - \langle g^2 \rangle), \quad (2.2)$$

where γ_1 and γ_2 are the model dependent constant parameters. In this paper, we adopt the convention in Ref. [41], where \mathcal{S} is defined to be the density contrast of neutrino in the synchronous gauge of CDM, with curvature perturbations being set to vanish. The two-point correlation and the cross-correlation functions are

$$\langle \mathcal{R}(\mathbf{x})\mathcal{R}(0) \rangle = \langle \mathcal{R}_G(\mathbf{x})\mathcal{R}_G(0) \rangle + 2\gamma_1^2 \langle g(\mathbf{x})g(0) \rangle^2, \quad (2.3)$$

$$\langle \mathcal{R}(\mathbf{x})\mathcal{S}(0) \rangle = 2\gamma_1\gamma_2 \langle g(\mathbf{x})g(0) \rangle^2, \quad (2.4)$$

$$\langle \mathcal{S}(\mathbf{x})\mathcal{S}(0) \rangle = 2\gamma_2^2 \langle g(\mathbf{x})g(0) \rangle^2, \quad (2.5)$$

and their Fourier transformations have the following form:

$$P_{SS}(k) = 2\gamma_2^2 \int \frac{d^3k_1}{(2\pi)^3} P_g(k_1) P_g(|\mathbf{k} - \mathbf{k}_1|), \quad (2.6)$$

$$P_{\mathcal{R}\mathcal{R}}(k) = P_G(k) + \frac{\gamma_1^2}{\gamma_2^2} P_{SS}(k), \quad (2.7)$$

$$P_{\mathcal{R}\mathcal{S}}(k) = \frac{\gamma_1}{\gamma_2} P_{SS}(k), \quad (2.8)$$

where we define the power spectra P_G and P_g for the above two Gaussian fields,

$$P_G(k) = \int \frac{d^3k}{(2\pi)^3} e^{-i\mathbf{k}\cdot\mathbf{x}} \langle \mathcal{R}_G(\mathbf{x})\mathcal{R}_G(0) \rangle, \quad (2.9)$$

$$P_g(k) = \int \frac{d^3k}{(2\pi)^3} e^{-i\mathbf{k}\cdot\mathbf{x}} \langle g(\mathbf{x})g(0) \rangle. \quad (2.10)$$

³ While we can also consider weakly non-Gaussian (i.e. local-type) NID perturbations, difference in results (i.e. μ and μT cross-correlation) are rather trivial due to the similarity in the transfer functions. Indeed, as we will discuss at the ends of Section 3.1 and 4, both μ -distortion and μT cross-correlation change only by a constant multiplicative factor from the adiabatic case [23].

Dimensionless power spectra are also defined as usual, i.e. $\mathcal{P}(k) = \frac{k^3}{2\pi^2} P(k)$ for each perturbations. Since \mathcal{P}_G is a power spectrum of the Gaussian curvature perturbation, we can parameterize it as

$$\mathcal{P}_G(k) = A_G \left(\frac{k}{k_0} \right)^{n_s-1}, \quad (2.11)$$

where $A_G = 2.196 \times 10^{-9}$ and $n_s = 0.96$ [3], with $k_0 = 0.05 \text{ Mpc}^{-1}$ being the pivot scale. The fraction of the isocurvature perturbations is given by

$$\beta_{\text{iso}} := \frac{\mathcal{P}_{SS}(k_0)}{\mathcal{P}_{\mathcal{RR}}(k_0) + \mathcal{P}_{SS}(k_0)}. \quad (2.12)$$

In the case with the neutrino density isocurvature mode, we already have the constraints $\beta_{\text{NID}} < 0.27$ or $\mathcal{P}_{SS}/\mathcal{P}_{\mathcal{RR}} < 0.37$ [3]. An ensemble average of a product of quantities defined as $\hat{F}(\mathbf{k}) = F_{\mathbf{k}}(\mathcal{R}_{\mathbf{k}} + f_{\mathbf{k}}\mathcal{S}_{\mathbf{k}})$ is calculated as

$$\langle \hat{F}(\mathbf{k}) \hat{F}(\mathbf{k}') \rangle = (2\pi)^3 \delta^{(3)}(\mathbf{k} + \mathbf{k}') F_{\mathbf{k}} F_{-\mathbf{k}} \left[P_G(k) + \left(f_{\mathbf{k}} f_{-\mathbf{k}} + \frac{\gamma_1}{\gamma_2} (f_{\mathbf{k}} + f_{-\mathbf{k}}) + \frac{\gamma_1^2}{\gamma_2^2} \right) P_{SS}(k) \right], \quad (2.13)$$

where $F_{\mathbf{k}}$ and $F_{\mathbf{k}} f_{\mathbf{k}}$ are transfer functions from the curvature perturbation and the isocurvature perturbation. Here we could integrate (2.6) explicitly by the use of the Feynman parameters and obtain

$$\mathcal{P}_{SS}(k) = \gamma_2^2 \mathcal{P}_g^2(k) \frac{2^{1-n_g} \pi \Gamma\left(\frac{5}{2} - n_g\right) \Gamma\left(\frac{n_g-1}{2}\right)}{\Gamma^2\left(2 - \frac{n_g}{2}\right) \Gamma\left(\frac{n_g}{2}\right)}, \quad \text{for } 1 < n_g < 2.5, \quad (2.14)$$

where we assume that \mathcal{P}_g is a power of wavenumber with a spectral index n_g , i.e. $\mathcal{P}_g(k) = \mathcal{P}_g(k_0)(k/k_0)^{n_g-1}$. We can see that $\mathcal{P}_{SS}(k) \propto \mathcal{P}_g^2(k)$, so that $\mathcal{P}_{SS}(k)$ can be parametrized as

$$\mathcal{P}_{SS}(k) = \mathcal{P}_{SS}(k_0) \left(\frac{k}{k_0} \right)^{2n_g-2}. \quad (2.15)$$

This suggests that the blue tilted original Gaussian field induces bluer isocurvature. $\mathcal{P}_{SS}(k_0)$ apparently has the IR logarithmic divergence at $n_g = 1$, therefore, let us introduce an IR cut-off which is motivated by the horizon size $L = 14 \text{ Gpc}$ to obtain a physically reasonable value for the power spectrum. For the almost flat spectrum, most contributions are from the two IR regions, and they are equivalent by the translation and variable transformation (see Fig. 1). Then we can combine these regions into one and obtain the following form from (2.6) and obtain

$$\begin{aligned} \mathcal{P}_{SS}(k_0) &\simeq 4\gamma_2^2 \mathcal{P}_g^2(k_0) \int_{1/(k_0 L)}^{k_{\text{max}}/k_0} d(\ln t) t^{n_g-1} \\ &= \frac{4}{n_g-1} \gamma_2^2 \mathcal{P}_g^2(k_0) \left[\left(\frac{k}{k_0} \right)^{n_g-1} \right]_{L^{-1}}^{k_{\text{max}}}, \end{aligned} \quad (2.16)$$

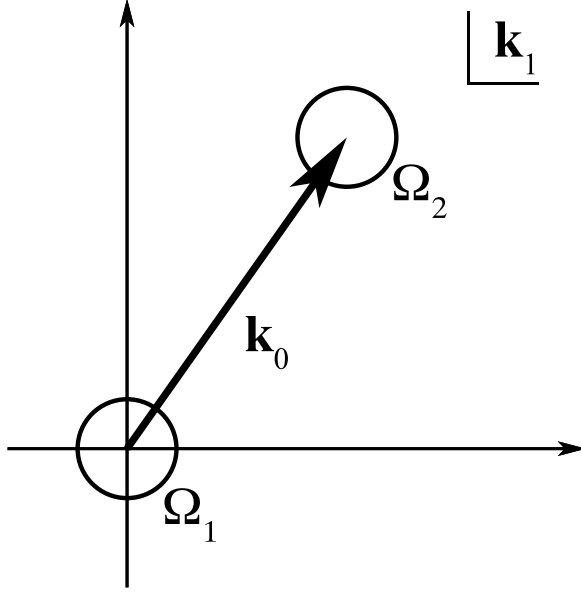


Figure 1. The schematic diagram of IR regions for the convolutional integration of $\mathcal{P}_{SS}(k_0)$. There are two IR singularities at $\mathbf{k}_1 = 0$ and \mathbf{k}_0 , and the IR regions around them, Ω_1 and Ω_2 , are equivalent as they can be interchanged by variable transformation. It can be seen the maximum radii of them, k_{\max} , are about $k_0/2$. Hereafter we take $k_{\max} = k_0$ for simplicity.

where k_{\max} is the upper limit of the IR region. Expanding by $n_g - 1$, we obtain the expression around the flat spectrum

$$\mathcal{P}_{SS}(k_0) \sim 4\gamma_2^2 \mathcal{P}_g^2(k_0) \log(k_{\max} L) \left[1 + \frac{n_g - 1}{2} \log\left(\frac{k_{\max}}{k_0^2 L}\right) + \dots \right]. \quad (2.17)$$

The IR singular points which are originally at $\mathbf{k}_1 = 0$, \mathbf{k}_0 are separated by the distance of k_0 . Therefore the radii of the IR regions can be taken up to about $k_0/2$ at most. For simplicity, we take $k_{\max} = k_0$ hereafter. Fig. 2 shows the comparison of the exact formula with the one with a IR cut-off. We can see that they are in good agreement up to $n_g \simeq 1.7$.

Three-point correlation functions are defined in the same manner and their bispectra can be obtained by the Fourier transformation. For instance, the bispectrum of the isocurvature perturbations are written as follows.

$$\begin{aligned} B_{SSS}(k_1, k_2, k_3) &= \int d^3x \int d^3y e^{-i\mathbf{k}\cdot\mathbf{x}} e^{-i\mathbf{k}\cdot\mathbf{y}} \langle \mathcal{S}(\mathbf{x}) \mathcal{S}(\mathbf{y}) \mathcal{S}(0) \rangle \\ &= 8\gamma_2^3 \int \frac{d^3q}{(2\pi)^3} P_g(q) P_g(|\mathbf{q} - \mathbf{k}_1|) P_g(\mathbf{q} - \mathbf{k}_1 - \mathbf{k}_2). \end{aligned} \quad (2.18)$$

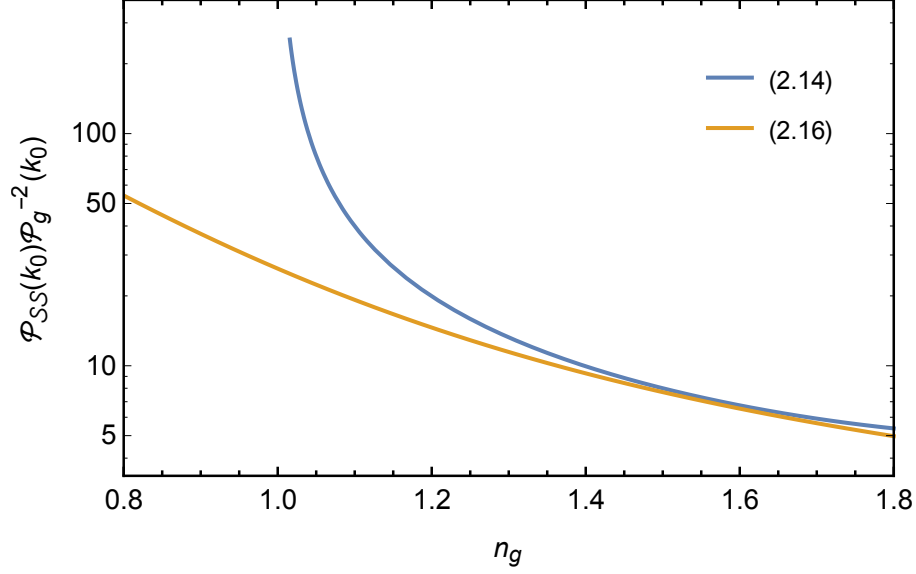


Figure 2. g^2 isocurvature power spectrum at pivot scale $k_0 = 0.05 \text{Mpc}^{-1}$ in units of $\mathcal{P}_g^2(k_0)$ with $\gamma_2 = 1$. In the latter sections, we will assume $n_g \lesssim 1.5$ in which the IR formulae can be used safely.

By the use of the B_{SSS} , the other bispectra are given by

$$B_{\mathcal{R}\mathcal{R}\mathcal{R}}(k_1, k_2, k_3) = \left(\frac{\gamma_1}{\gamma_2}\right)^3 B_{SSS}(k_1, k_2, k_3), \quad (2.19)$$

$$B_{\mathcal{R}\mathcal{R}\mathcal{S}}(k_1, k_2, k_3) = \left(\frac{\gamma_1}{\gamma_2}\right)^2 B_{SSS}(k_1, k_2, k_3), \quad (2.20)$$

$$B_{\mathcal{R}SS}(k_1, k_2, k_3) = \frac{\gamma_1}{\gamma_2} B_{SSS}(k_1, k_2, k_3). \quad (2.21)$$

Then a triple product of $\hat{F}(\mathbf{k})$ also has the following form:

$$\begin{aligned} & \langle \hat{F}(\mathbf{k}_1) \hat{F}(\mathbf{k}_2) \hat{F}(\mathbf{k}_3) \rangle \\ &= (2\pi)^3 \delta^3(\mathbf{k}_1 + \mathbf{k}_2 + \mathbf{k}_3) B_{SSS}(k_1, k_2, k_3) F_{\mathbf{k}_1} F_{\mathbf{k}_2} F_{\mathbf{k}_3} \\ & \times \left(f_{\mathbf{k}_1} f_{\mathbf{k}_2} f_{\mathbf{k}_3} + \frac{\gamma_1}{\gamma_2} (f_{\mathbf{k}_1} f_{\mathbf{k}_2} + f_{\mathbf{k}_2} f_{\mathbf{k}_3} + f_{\mathbf{k}_3} f_{\mathbf{k}_1}) + \frac{\gamma_1^2}{\gamma_2^2} (f_{\mathbf{k}_1} + f_{\mathbf{k}_2} + f_{\mathbf{k}_3}) + \frac{\gamma_1^3}{\gamma_2^3} \right). \end{aligned} \quad (2.22)$$

B_{SSS} also has IR singularities, and here we treat them in the same way as the power spectrum. Let us assume a squeezed configuration, which we will consider in the latter sections. Let the wavenumbers satisfy $k_1 \ll k_2 \simeq k_3$. In this limit, the contributions of two IR regions which include k_1 are dominant (see Fig. 3). Therefore (2.18) can be written as

$$\begin{aligned} B_{SSS}(k_1, k_2, k_3) &\simeq \frac{8}{n_g - 1} \gamma_2^3 \mathcal{P}_g(k_0) \left[\left(\frac{k}{k_0} \right)^{n_g - 1} \right]_{L^{-1}}^{k_{\max}} \\ &\times [P_g(k_1) P_g(k_2) + P_g(k_1) P_g(k_3)], \quad \text{for } k_1 \ll k_2, k_3, \end{aligned} \quad (2.23)$$

where $k_{\max} \lesssim k_1$ and we will use $k_{\max} = k_1$ hereafter. Here we also introduce IR cut-off to be the current horizon size $\sim L$.

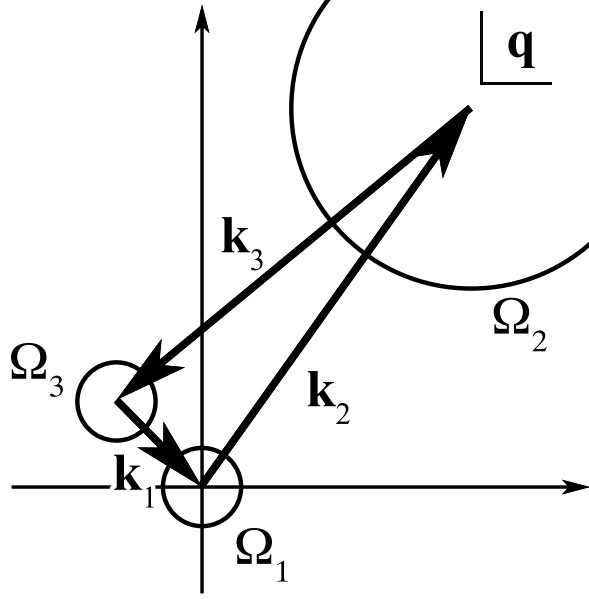


Figure 3. The IR regions of the integration for the bispectrum in the squeezed limit ($k_1 \ll k_2, k_3$). Since $P_g(k_1) \gg P_g(k_2), P_g(k_3)$ in this case, the contributions from Ω_1 and Ω_3 , which are approximately proportional to $P_g(k_1)P_g(k_2)$ and $P_g(k_1)P_g(k_3)$, are much larger than that from Ω_2 , which are approximately proportional to $P_g(k_2)P_g(k_3)$. Therefore we can consider the expansions of power spectrum only in Ω_1 and Ω_3 . At this time, the upper limit of these IR regions is around $k_1/2$. From now on, we take $k_{\max} = k_1$.

3 CMB μ -distortion

3.1 Homogeneous distortions

We usually assume that the photon system is locally thermal equilibrium in the early universe. In other words, the photon fluid has generally local Bose-Einstein distribution function defined as

$$f(\mathbf{x}, \omega) = \frac{1}{e^{\frac{\omega}{T_{\text{BE}}(\mathbf{x})} + \mu(\mathbf{x})} - 1}, \quad (3.1)$$

where \mathbf{x} and ω are spacetime point and frequency, respectively. Note that the temperature parameter of the Bose-Einstein distribution function T_{BE} is different from that of Planck distribution function T_{pl} . Assuming that the deviations from the Planck distribution function are induced by the mixing of different local blackbodies, $T_{\text{BE}} - T_{\text{pl}}$ and μ are the second-order quantities of the first-order dimensionless temperature perturbation defined as [27]

$$\Theta(\mathbf{x}) = \frac{T_{\text{pl}}(\mathbf{x}) - \langle T_{\text{pl}} \rangle}{\langle T_{\text{pl}} \rangle}. \quad (3.2)$$

Then, using the conservation laws of both average energy and number, we can derive the evolution equation for the averaged μ -distortion as follows [16]

$$\frac{d}{d\eta} \langle \mu \rangle = -\frac{\langle \mu \rangle}{t_\mu} - 1.4 \times 4 \left\langle \Theta \frac{d\Theta}{d\eta} \right\rangle + \mathcal{O}(\Theta^3), \quad (3.3)$$

where η is conformal time and the first term is added by hand to take into account the effect of the process which do not conserve the number of photon such as the double Compton effect or electron-positron pair annihilation. t_μ is the time-scale of decreasing of the chemical potential by the above processes, which become ineffective at $z \lesssim 2 \times 10^6$ [28, 29]. $d\Theta/d\eta$ is immediately calculated by linear Boltzmann equations. Here let us follow the notation in Ma and Bertschinger [30]. In Fourier space, the brightness functions for intensity and linear polarization are given by

$$F_\gamma = \frac{\int q^2 dq q f^{(0)}(q) \Psi}{\int q^2 dq q f^{(0)}(q)}, \quad (3.4)$$

$$G_\gamma = \frac{\int q^2 dq q f^{(0)}(q) \Psi_P}{\int q^2 dq q f^{(0)}(q)}, \quad (3.5)$$

where q is comoving momentum and $f^{(0)}$ is the background Planck distribution function. Ψ and Ψ_P are fractional perturbations in $\rho_{11} + \rho_{22}$ and $\rho_{11} - \rho_{22}$ of the photon density matrix, respectively. We expand these quantities with respect to multipoles as $F_\gamma = \sum_{l=0} (-i)^l (2l+1) P_l(\lambda) F_{\gamma l}$ to obtain the solutions order by order. To the linear order, $F_\gamma = 4\Theta$ is always satisfied. Then we can derive the following formulae for the μ -distortion [31]

$$\begin{aligned} \langle \mu \rangle = & 1.4 \cdot \frac{1}{4} \int_0^{\eta_f} d\eta' \mathcal{J}_{DC}(\eta') \int d(\ln k) \left[\mathcal{P}_G(k) + \left(f + \frac{\gamma_1}{\gamma_2} \right)^2 \mathcal{P}_{SS}(k) \right] \\ & \times n_e \sigma_T a \left[\frac{3}{4} (F_{\gamma 1} - F_{b1})^2 - \frac{F_{\gamma 2}}{2} (-9F_{\gamma 2} + G_{\gamma 2} + G_{\gamma 0}) + \sum_{l \geq 3} (2l+1) F_{\gamma l} F_{\gamma l} \right], \end{aligned} \quad (3.6)$$

where \mathcal{J}_{DC} is a window function induced by double Compton scattering and η_f is the end time of μ era. F_{b1} is the velocity perturbation of baryons. Here, $f = -R_\nu/(4R_\gamma)$ with $R_\nu = \rho_\nu/(\rho_\nu + \rho_\gamma)$ and $R_\gamma = 1 - R_\nu$ is the ratio of the NID mode to the adiabatic mode and the transfer functions have the same form with (2.13) [41]. We replace $F_{\gamma 1} \rightarrow F_{\gamma 1} - F_{b1}$ to manifest gauge invariance of the first term, which can be omitted in the radiation dominated period. Note that Legendre coefficients and f only depend on the magnitude of \mathbf{k} . In the tight coupling regime, we can approximately solve Boltzmann equations for the photon sector analytically. In the case with adiabatic condition, the solution is given by [42]

$$F_{\gamma 1} \sim -\frac{4}{\sqrt{3}} \sin(kr_s) \exp\left(-\frac{k^2}{k_D^2}\right), \quad (3.7)$$

where r_s is the sound horizon and k_D is the Silk damping scale. In the tight coupling regime we can write $G_{\gamma 0} + G_{\gamma 2} = 3F_{\gamma 2}/2$, then (3.6) can be approximate as

$$\begin{aligned} \langle \mu \rangle = & -2.8 \int_0^{\eta_f} d\eta \mathcal{J}_{DC}(\eta) \int d(\ln k) \left[\mathcal{P}_G(k) + \left(f + \frac{\gamma_1}{\gamma_2} \right)^2 \mathcal{P}_{SS}(k) \right] \partial_\eta \exp\left(-2\frac{k^2}{k_D^2}\right) \\ \sim & -2.8 \int d(\ln k) \left[\mathcal{P}_G(k) + \left(f + \frac{\gamma_1}{\gamma_2} \right)^2 \mathcal{P}_{SS}(k) \right] \left[\exp\left(-2\frac{k^2}{k_D^2}\right) \right]_i^f, \end{aligned} \quad (3.8)$$

where we have used the relation $F_{\gamma 2} = 8kF_{\gamma 1}/(15\dot{\tau})$ and replace $\sin^2(kr_s)$ with $1/2$, and in addition we have adopted the relation $\partial_\eta k_D^{-2} = -8/(45\dot{\tau})$ in the limit of full radiation

domination. Let us divide $\langle \mu \rangle$ into parts originating from \mathcal{R}_G and g^2 , that is, $\langle \mu \rangle = \langle \mu \rangle_G + \langle \mu \rangle_{g^2}$. Then (3.8) yields

$$\begin{aligned}\langle \mu \rangle_G &= 2.8 \mathcal{P}_G(k_0) \log \left(\frac{k_{Di}}{k_{Df}} \right) \left[1 + \frac{n_s - 1}{2} \left(\log \left(\frac{k_{Di} k_{Df}}{2k_0^2} \right) - \mathbf{C} \right) + \dots \right] \\ &= 3.36 \times 10^{-8} [1 + 8.91(n_s - 1) + \dots],\end{aligned}\quad (3.9)$$

where $\mathbf{C} = 0.577\dots$ is Euler-Mascheroni constant and $\log(k_{Di}/k_{Df}) \simeq 5.477$. If we take into account terms of $\mathcal{O}(n_s - 1)$ with $n_s = 0.96$, $\langle \mu \rangle$ becomes 2.2×10^{-8} , which is consistent with the values derived in the previous works [10, 13–15]. The second order correction is smaller than 10%. Another contribution from g^2 can be calculated as

$$\begin{aligned}\langle \mu \rangle_{g^2} &= 1.4 \mathcal{P}_{\mathcal{SS}}(k_0) \left(\frac{R_\nu}{4R_\gamma} + \frac{\gamma_1}{\gamma_2} \right)^2 \left[\left(\frac{k_D}{\sqrt{2}k_0} \right)^{2n_g-2} \right]_f^i \Gamma(n_g - 1) \\ &= \frac{5.6\gamma_2^2 \mathcal{P}_g^2(k_0)}{n_g - 1} \left(\frac{R_\nu}{4R_\gamma} + \frac{\gamma_1}{\gamma_2} \right)^2 \left[\left(\frac{k}{k_0} \right)^{n_g-1} \right]_{L^{-1}}^{k_{\max}} \left[\left(\frac{k_D}{\sqrt{2}k_0} \right)^{2n_g-2} \right]_f^i \Gamma(n_g - 1),\end{aligned}\quad (3.10)$$

where we have used (2.17). Suppose that uncorrelated case with $\gamma_1 = 0$ and $\gamma_2 = 1$, expanding around the flat case, we obtain

$$\langle \mu \rangle_{g^2}^{\text{uncor}} \simeq 12.1 \mathcal{P}_g^2(k_0) \left[1 + 13.9(n_g - 1) + \dots \right], \quad (3.11)$$

where $k_{\max} = k_0$. Fig. 4 shows $\langle \mu \rangle_{g^2}^{\text{uncor}}$ as a function of n_g . For \mathcal{S} not to dominate \mathcal{R} , we should impose $\mathcal{P}_{\mathcal{SS}}(k_0) \sim \mathcal{P}_g^2(k_0) \lesssim 10^{-10}$ (we obtain similar constraints from the CMB angular bispectrum and see Appendix A for details). For example, assuming $\mathcal{P}_g(k_0) \sim 10^{-5}$, it can be shown from (3.11) that $\langle \mu \rangle_{g^2}^{\text{uncor}} \sim 10^{-9}$ for the case of flat spectrum $n_g \sim 1$. As shown in Fig. 4, if we consider the blue-tilted power spectrum of g , we can realize the large enhancement of $\langle \mu \rangle$. From this figure, by employing the COBE FIRAS constraint, that is, $\mu < 9 \times 10^{-5}$, we find an upper limit on n_g as $n_g \lesssim 1.5$.

Incidentally, the μ -distortion originating from almost Gaussian uncorrelated NID mode is also calculated straightforwardly and the difference from the case of the adiabatic perturbation is only from that of the transfer functions of them. Specifically, the μ -distortion from the isocurvature mode becomes $\mathcal{O}(0.01)$ times smaller than that of the standard adiabatic perturbation case (see [26] for more details).

3.2 Inhomogeneous distortions

In the case with inhomogeneous distortions, (3.3) does not work since the equation is a result of conservation laws in the homogeneous and isotropic background. In other words, the quantities in the equation are globally averaged. Therefore, generally we should consider local conservation laws of energy-momentum tensor $\nabla_\mu T^{\mu\nu} = 0$ and number flux $\nabla_\mu N^\mu = 0$ to compute inhomogeneous distortions [43]. Nevertheless approximately we can just remove $\langle \dots \rangle$ of (3.3) since the thermodynamic valuables are locally averaged quantities. Therefore we again use (3.8) with the slight change

$$\int d(\ln k) \mathcal{P}_{\mathcal{XY}}(k) \rightarrow \int \frac{d^3 k}{(2\pi)^3} \frac{d^3 k'}{(2\pi)^3} e^{i(\mathbf{k}+\mathbf{k}')\cdot\mathbf{x}} \mathcal{X}(\mathbf{k}) \mathcal{Y}(\mathbf{k}') 5P_2(\hat{\mathbf{k}}\cdot\mathbf{n}) P_2(\hat{\mathbf{k}}'\cdot\mathbf{n}), \quad \text{with } \mathcal{X}, \mathcal{Y} = \mathcal{R}, \mathcal{S}, \quad (3.12)$$

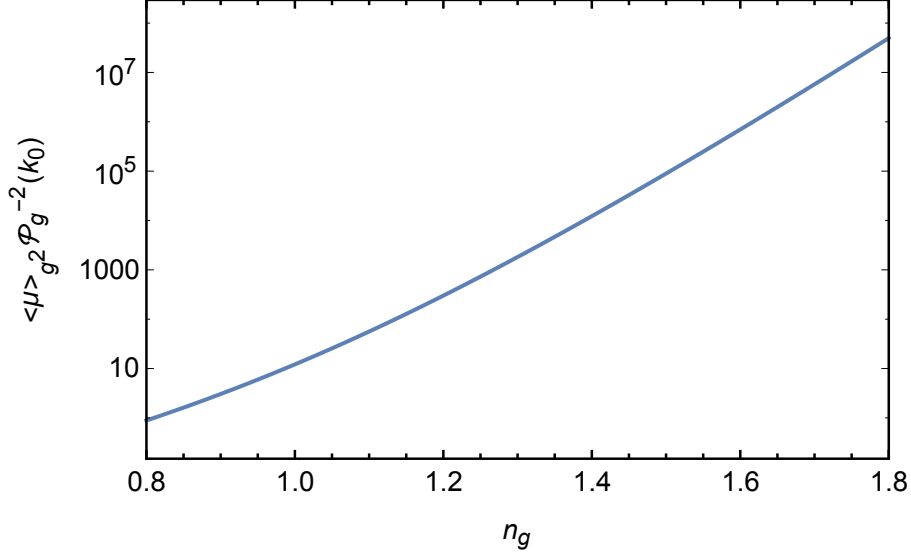


Figure 4. n_g v.s. $\langle \mu \rangle_g^{\text{uncor}}$ in units of $\mathcal{P}_g^2(k_0)$. Here γ_1 and γ_2 are set to zero and unity, respectively.

where \hat{k} and \hat{k}' are unit vector of \mathbf{k} and \mathbf{k}' . \mathbf{n} is a tangent vector of the line-of-sight of the photons. Then we obtain the μ distortion in Fourier space as follows:

$$\begin{aligned} \mu(\eta_f, \mathbf{k}) = & 16\alpha \int \frac{d^3 k_1}{(2\pi)^3} \left[\mathcal{R}_{G\mathbf{k}_1} \mathcal{R}_{G\mathbf{k}_2} + \left(\frac{R_\nu}{4R_\gamma} + \frac{\gamma_1}{\gamma_2} \right)^2 \mathcal{S}_{\mathbf{k}_1} \mathcal{S}_{\mathbf{k}_2} \right] \\ & \times 5P_2(\hat{k}_1 \cdot \mathbf{n}) P_2(\hat{k}_2 \cdot \mathbf{n}) \langle \sin k_1 r_s \sin k_2 r_s \rangle_p \left[\exp \left(-\frac{k_1^2 + k_2^2}{k_D^2} \right) \right]_f^i, \end{aligned} \quad (3.13)$$

where $\alpha = -1.4 \times 1/4$, $\mathbf{k}_2 = \mathbf{k} - \mathbf{k}_1$ and $\langle \cdots \rangle_p$ is a periodic average.

4 μT angular cross-correlation

The harmonic coefficients of observed anisotropies in Θ and μ can be written as

$$a_{T,lm} = \int d\mathbf{n} Y_{lm}^*(\mathbf{n}) \Theta(\eta_0, \mathbf{x}, \mathbf{n}), \quad (4.1)$$

$$a_{\mu,lm} = \int d\mathbf{n} Y_{lm}^*(\mathbf{n}) \mu(\eta_0, \mathbf{x}, \mathbf{n}), \quad (4.2)$$

where η_0 is the conformal time today and \mathbf{n} is a line-of-sight. Without loss of generality, we can take $\mathbf{x} = 0$. Then the angular power spectrum of the μT cross-correlation function is defined as usual,

$$C_l^{\mu T} = \frac{1}{2l+1} \sum_m \langle a_{\mu,lm}^* a_{T,lm} \rangle. \quad (4.3)$$

In Fourier space, the temperature perturbations are

$$\Theta(\eta, \mathbf{k}, \mathbf{n}) = \Theta^{\mathcal{R}}(\eta; k, \lambda) \mathcal{R}_{\mathbf{k}} + \Theta^{\mathcal{S}}(\eta; k, \lambda) \mathcal{S}_{\mathbf{k}}, \quad (4.4)$$

where λ is the cosine between \mathbf{k} and \mathbf{n} . On the other hand, the μ -distortion is written as

$$\mu(\eta, \mathbf{k}, \mathbf{n}) = \Delta_\mu(\eta; \eta_f, k, \lambda) \mu(\eta_f, \mathbf{k}), \quad (4.5)$$

where $\mu(\eta_f, \mathbf{k})$ is what we calculated in the last section and the transfer function is given in Ref. [43]. Substituting (4.4) and (3.13) into (4.1) and (4.2), we obtain

$$a_{T,lm} = 4\pi(-i)^l \int \frac{d^3k}{(2\pi)^3} Y_{lm}^*(\hat{k}) \left[\Theta_l^{\mathcal{R}}(\eta_0, k) \mathcal{R}_{G\mathbf{k}} + \left(\Theta_l^{\mathcal{S}}(\eta_0, k) + \frac{\gamma_1}{\gamma_2} \Theta_l^{\mathcal{R}}(\eta_0, k) \right) \mathcal{S}_{\mathbf{k}} \right], \quad (4.6)$$

$$a_{\mu,lm} = 4\pi(-i)^l \cdot 16\alpha \int \frac{d^3k}{(2\pi)^3} \frac{d^3k_1}{(2\pi)^3} Y_{lm}^*(\hat{k}) \Delta_{\mu l}(\eta_0, k) \langle \sin k_1 r \sin k_2 r \rangle_p 5P_2(\hat{k}_1 \cdot \mathbf{n}) P_2(\hat{k}_2 \cdot \mathbf{n}) \\ \times \left[\exp \left(-\frac{k_1^2 + k_2^2}{k_D^2} \right) \right]_f^i \left[\mathcal{R}_{G\mathbf{k}_1} \mathcal{R}_{G\mathbf{k}_2} + \left(\frac{R_\nu}{4R_\gamma} + \frac{\gamma_1}{\gamma_2} \right)^2 \mathcal{S}_{\mathbf{k}_1} \mathcal{S}_{\mathbf{k}_2} \right], \quad (4.7)$$

where we define $\hat{k} = \mathbf{k}/k$, and $\Theta_l^X (X = \mathcal{R}, \mathcal{S})$ and $\Delta_{\mu l}$ are the Legendre coefficients of the transfer functions. On large angular scales where the Sachs-Wolfe effect is dominant, Θ_l 's are given by

$$\Theta_l(\eta_0, k) \sim [\Theta_0(\eta_*) + \psi(\eta_*)] j_l(k(\eta_0 - \eta_*)), \quad (4.8)$$

where η_* is conformal time at recombination and ψ is the gravitational potential in the conformal Newtonian gauge. $\Theta_0(\eta_*) + \psi(\eta_*)$ depends on the initial conditions. Using the numerical code CLASS [44], $\Theta_0(\eta_*) + \psi(\eta_*) \sim -0.24$ for the adiabatic perturbation and $\Theta_0(\eta_*) + \psi(\eta_*) \sim -0.175$ for the neutrino isocurvature density mode, respectively. $\Delta_{\mu l}$ is also given by the line-of-sight integral method as shown in Ref. [43]. Using the above equations, μT angular power spectrum is obtained as

$$|C_l^{\mu T}| = \frac{(4\pi)^2 \alpha}{2l+1} \left(0.175 + 0.24 \frac{\gamma_1}{\gamma_2} \right) \left(\frac{R_\nu}{R_\gamma} + \frac{4\gamma_1}{\gamma_2} \right)^2 \int \frac{d^3k d^3k_1 d^3k_2}{(2\pi)^9} \sum_{m=-l}^l Y_{lm}^*(\hat{k}) Y_{lm} \left(\frac{\mathbf{k}_1 + \mathbf{k}_2}{|\mathbf{k}_1 + \mathbf{k}_2|} \right) \\ \times 5P_2(\hat{k}_1 \cdot \mathbf{n}) P_2(\hat{k}_2 \cdot \mathbf{n}) \langle \mathcal{S}_{\mathbf{k}} \mathcal{S}_{\mathbf{k}_1}^* \mathcal{S}_{\mathbf{k}_2}^* \rangle j_l(k\eta_0) j_l(|\mathbf{k}_1 + \mathbf{k}_2|\eta_0) \langle \sin k_1 r_s \sin k_2 r_s \rangle_p \left[\exp \left(-\frac{k_1^2 + k_2^2}{k_D^2} \right) \right]_f^i, \quad (4.9)$$

where r_s is the sound horizon and $\eta_0 \gg \eta_*$. The three-point function $\langle \mathcal{S} \mathcal{S} \mathcal{S} \rangle$ is nonzero since \mathcal{S} is non-Gaussian. From the reality condition, we obtain

$$\langle \mathcal{S}_{\mathbf{k}} \mathcal{S}_{\mathbf{k}_1}^* \mathcal{S}_{\mathbf{k}_2}^* \rangle = \langle \mathcal{S}_{\mathbf{k}} \mathcal{S}_{-\mathbf{k}_1} \mathcal{S}_{-\mathbf{k}_2} \rangle = (2\pi)^3 \delta^{(3)}(\mathbf{k} - \mathbf{k}_1 - \mathbf{k}_2) B_{\mathcal{S} \mathcal{S} \mathcal{S}}(k, k_1, k_2). \quad (4.10)$$

Let us consider a transformation $\mathbf{k}_\pm = \mathbf{k}_1 \pm \mathbf{k}_2$. Since we will concentrate on low- l , the integrations of \mathbf{k} and \mathbf{k}_+ are negligible except around CMB scales $k = k_+ \sim k_0$, because of the behaviour of the spherical Bessel functions. On the other hand, due to the exponential suppression factor the contribution around $k_1^2 + k_2^2 \sim k_D^2 \gg k_0$ is dominant. Therefore, from $k_+^2 + k_-^2 = 2(k_1^2 + k_2^2) \gg k_+^2$, we obtain a hierarchical relation $k_- \gg k_+$. At this time, since $k_1 \sim k_2 \sim k_-/2$, we can approximate the periodic average $\langle \sin k_1 r \sin k_2 r \rangle_p$ by 1/2. From the above results, noting that the Jacobian of coordinate transformation to \mathbf{k}_\pm is 1/8 and we consider the squeezed configuration now, we obtain

$$B_{SSS}(k_+, k_-/2, k_-/2) \sim \frac{2\pi^2}{k_+^3} \frac{2\pi^2}{(k_-/2)^3} \left(\frac{k_+}{k_0}\right)^{n_g-1} \left(\frac{k_-/2}{k_0}\right)^{n_g-1} \frac{16\mathcal{P}_g^3(k_0)}{n_g-1} \left[\left(\frac{k}{k_0}\right)^{n_g-1}\right]_{L^{-1}}^{k_{\max}}, \quad (4.11)$$

with use of (2.23). Finally we have the following form

$$|C_l^{\mu T}| \sim 0.583 \left(1 + 1.4 \frac{\gamma_1}{\gamma_2}\right) \left(1 + 5.8 \frac{\gamma_1}{\gamma_2}\right)^2 \frac{\gamma_2^3 \mathcal{P}_g^3(k_0)}{n_g-1} \left[\left(\frac{k}{k_0}\right)^{n_g-1}\right]_{L^{-1}}^{k_{\max}} \times \left[\left(\frac{\sqrt{2}k_D}{k_0^2 L}\right)^{n_g-1}\right]_f^i \frac{\Gamma(l + \frac{n_g}{2} - \frac{1}{2}) \Gamma(3 - n_g) \Gamma(\frac{n_g-1}{2})}{\Gamma(l + \frac{5}{2} - \frac{n_g}{2}) \Gamma^2(2 - \frac{n_g}{2})}, \quad (4.12)$$

where we have used $P_2(-\hat{k}_- \cdot \mathbf{n}) = P_2(\hat{k}_- \cdot \mathbf{n})$ in the integration with respect to \hat{k}_- and $\eta_0 = L$. For the flat and uncorrelated spectrum with $\mathcal{P}_g \sim 10^{-5}$, which would be marginally allowed by CMB bispectrum from Planck (See Appendix A for the Planck forecast), and taking $k_{\max} = k_0$, we obtain $|l(l+1)C_l^{\mu T}| \sim 10^{-14}$. This level of signal corresponds to $f_{\text{NL}}^{\text{loc}} \sim 100$ in the case of the local-type non-Gaussianity in adiabatic perturbations [23], which is 10 times smaller than the expected sensitivity of PIXIE and comparable to that of PRISM. For $l = 10$ with $k_{\max} = k_0$ and $\gamma_1 = 0$,

$$\frac{(10 \cdot 11) \times |C_{10}^{\mu T}|}{\mathcal{P}_g^3(k_0)} \sim 53.4 \left[1. + 1.75514(n_g - 1) + \dots\right]. \quad (4.13)$$

Fig. 5 shows that n_g -dependence of $110C_{10}^{\mu T} \mathcal{P}_g^{-3}(k_0)$. In the case with $n_g \sim 1.5$, the signal is almost 10 times bigger than that with the flat case, and can be also detected by PIXIE.

For the sake of completeness, let us consider the case with almost Gaussian neutrino isocurvature density mode, $\mathcal{S} = \mathcal{S}_G + f_{\text{NL}}^{\text{loc}, \nu}(\mathcal{S}_G^2 - \langle \mathcal{S}_G^2 \rangle)$. Local-type bispectrum of the uncorrelated isocurvature perturbation is parametrized as

$$B_{\mathcal{S}}(k_+, k_-/2, k_-/2) = -\frac{6}{5} f_{\text{NL}}^{\text{loc}, \nu} [P_{\mathcal{S}}(k_+) P_{\mathcal{S}}(k_-/2) + 2\text{perm.}] \sim -\frac{6 \times 2}{5} f_{\text{NL}}^{\text{loc}, \nu} P_{\mathcal{S}}(k_+) P_{\mathcal{S}}(k_-/2). \quad (4.14)$$

As discussed below (3.7) and (4.8), transfer functions of the adiabatic and NID modes differ only by a multiplicative constant factor. Thus by taking account this difference in the results of Ref. [23], we obtain

$$l(l+1)C_l^{\mu T} \lesssim 8.04 \times 10^{-19} f_{\text{NL}}^{\text{loc}, \nu} \left[1 + \left(5.37 + \frac{1}{l} + \frac{1}{l+1} + 2\psi^{(0)}(l)\right) \frac{n_s - 1}{2} + \dots\right], \quad (4.15)$$

where we have assumed $\beta_{\text{NID}} = 0.27$ and $\psi^{(0)}(x) = d \log \Gamma(x)/dx$ is a poly-gamma function. When $f_{\text{NL}} = f_{\text{NL}}^{\text{loc}, \nu}$, the μT cross-correlation from the non-Gaussian neutrino isocurvature perturbations should be 10^2 times smaller than that from the adiabatic ones calculated in Ref. [23]. However as is shown in Appendix A, the expected observational constraints on $f_{\text{NL}}^{\text{loc}, \nu}$ would be 10^4 at around 2σ level when $\beta_{\text{NID}} \simeq \mathcal{P}_{\mathcal{SS}}/\mathcal{P}_{\mathcal{RR}} = 10^{-1}$. When we take $f_{\text{NL}}^{\text{loc}, \nu}$

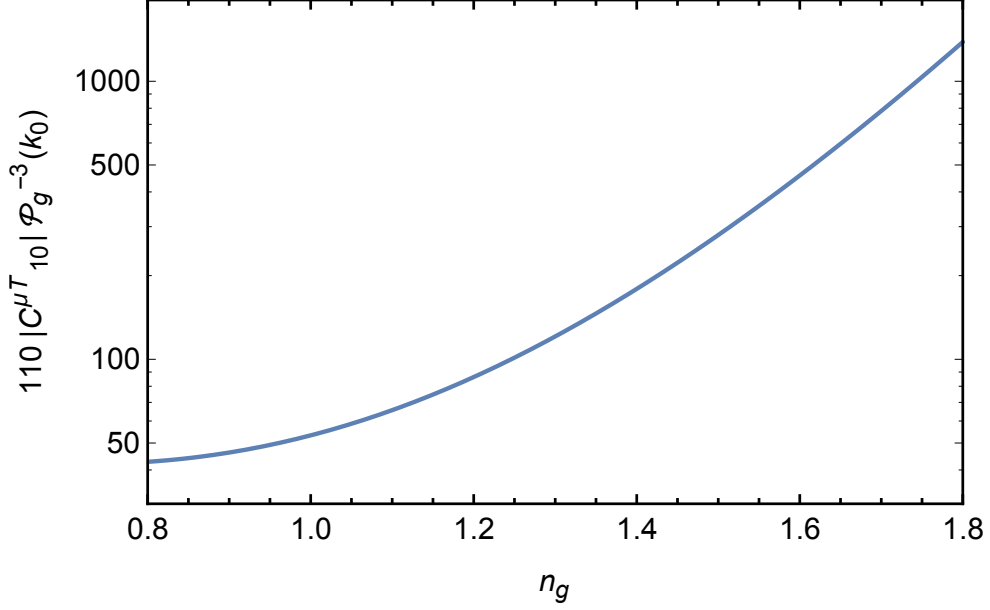


Figure 5. n_g dependence of $l(l+1)C_l^{\mu T}\mathcal{P}_g^{-3}(k_0)$ with $l = 10$.

to be 10^4 , the cross-correlation from the non-Gaussian neutrino isocurvature perturbations can be as large as that from local-type adiabatic ones with $f_{\text{NL}} = 100$. The size of signal here is the same as in the Gaussian-squared case, which we have presented before. This is by no means surprising since both the amplitudes of μT cross-correlation and the CMB bispectrum are determined by the primordial bispectrum, whose spectral shape can be approximated with the local-type one both in the cases of weakly non-Gaussian and Gaussian-squared isocurvature perturbations.

5 Conclusions

In this paper, we have calculated the mean μ -distortion and the cross-correlation of its anisotropy with primary CMB temperature one in the presence of non-Gaussian neutrino isocurvature perturbations. In particular, we have focused on the Gaussian-squared perturbations, and explicitly shown that the primordial bispectrum of Gaussian-squared type perturbations can be approximated by the local-type one. We have found that when the power spectrum of the isocurvature perturbations are nearly scale-invariant, the mean μ and the μT cross-correlation can be as large as 10^{-9} and 10^{-14} with the present constraints from CMB power spectrum and bispectrum on NID mode being satisfied. In particular, μT cross-correlation from NID perturbations is potentially observed by the PRISM surveys, which is contrastive to the cases of adiabatic local-type ones, which requires f_{NL} an order of magnitude larger than the upper bound from current CMB bispectrum measurements. If the power spectrum of isocurvature perturbations are allowed to be blue-tilted, the μT cross-correlation can be enhanced by an order of magnitude and expected to be observed by PIXIE.

Acknowledgments

We would like to thank Masahide Yamaguchi for the helpful discussions and comments. This work was supported by World Premier International Research Center Initiative (WPI Initiative), MEXT, Japan. Y.T. is supported by an Advanced Leading Graduate Course for Photon Science grant. T.S. is supported by the Academy of Finland grant 1263714.

A Constraints from CMB angular bispectrum

In this appendix, we summarize the Fisher matrix analysis of CMB bispectrum and forecast for the Planck constraints on non-Gaussian isocurvature perturbations, following Refs. [35, 45, 46]⁴. Let us start by generalizing the form of CMB anisotropies in (4.1) into

$$a_{lm}^P = 4\pi(-i)^l \int \frac{d^3k}{(2\pi)^3} \sum_X g_l^{XP}(k) Y_{lm}^*(\hat{k}) \mathcal{X}^X(\mathbf{k}), \quad (\text{A.1})$$

where \hat{k} is the unit vector of \mathbf{k} , X and P respectively represent types of initial perturbations and CMB anisotropies, i.e. X is either the adiabatic (\mathcal{R}) or neutrino isocurvature (\mathcal{S}) mode and P is either the temperature (T) or E-mode polarization (E) anisotropy. g_l^{XP} is the Legendre coefficient of the transfer function of P from X and numerically evaluated using the CAMB code [48]. The CMB bispectrum in harmonic space is given as

$$B_{l_1 m_1 l_2 m_2 l_3 m_3}^{P_1 P_2 P_3} \equiv \langle a_{l_1 m_1}^{P_1} a_{l_2 m_2}^{P_2} a_{l_3 m_3}^{P_3} \rangle. \quad (\text{A.2})$$

Given a primordial bispectrum

$$\langle \mathcal{X}^{X_1}(\mathbf{k}_1) \mathcal{X}^{X_2}(\mathbf{k}_2) \mathcal{X}^{X_3}(\mathbf{k}_3) \rangle = B^{X_1 X_2 X_3}(k_1, k_2, k_3) (2\pi)^3 \delta^{(3)}(\mathbf{k}_1 + \mathbf{k}_2 + \mathbf{k}_3), \quad (\text{A.3})$$

(A.2) can be rewritten as

$$\begin{aligned} B_{l_1 m_1 l_2 m_2 l_3 m_3}^{P_1 P_2 P_3} &= \sum_{X_1 X_2 X_3} \prod_{i=1}^3 \left[4\pi(-i)^{l_i} \int \frac{d^3k_i}{(2\pi)^3} g_{l_i}^{X_i P_i}(k_i) Y_{l_i m_i}^*(\hat{k}_i) \right] \\ &\quad \times B^{X_1 X_2 X_3}(k_1, k_2, k_3) (2\pi)^3 \delta^{(3)}(\mathbf{k}_1 + \mathbf{k}_2 + \mathbf{k}_3). \end{aligned} \quad (\text{A.4})$$

By Fourier transforming the delta function and using a formula for the partial wave decomposition

$$e^{i\mathbf{k}\cdot\mathbf{r}} = \sum_{lm} 4\pi i^l j_l(kr) Y_{lm}(\hat{k}) Y_{lm}^*(\hat{r}), \quad (\text{A.5})$$

(A.4) can be further recast into

$$B_{l_1 m_1 l_2 m_2 l_3 m_3}^{P_1 P_2 P_3} = \mathcal{G}_{l_1 l_2 l_3}^{m_1 m_2 m_3} b_{l_1 m_1 l_2 m_2 l_3 m_3}^{P_1 P_2 P_3}, \quad (\text{A.6})$$

where

$$b_{l_1 m_1 l_2 m_2 l_3 m_3}^{P_1 P_2 P_3} = \sum_{X_1 X_2 X_3} \int r^2 dr \prod_{i=1}^3 \left[\frac{2}{\pi} \int k_i^2 dk_i g_{l_i}^{X_i P_i}(k_i) j_{l_i}(k_i r) \right] B^{X_1 X_2 X_3}(k_1, k_2, k_3) \quad (\text{A.7})$$

⁴ We defer it for future work to derive constraints on non-Gaussian neutrino isocurvature perturbations from the actual Planck data here. Constraints from the WMAP data can be found in Ref. [47].

is the reduced bispectrum and

$$\mathcal{G}_{l_1 l_2 l_3}^{m_1 m_2 m_3} = \int d\hat{r} \prod_{i=1}^3 Y_{l_i m_i}^*(\hat{r}) \quad (\text{A.8})$$

is the Gaunt integral, which can be represented in terms of the Wigner-3j symbol as

$$\mathcal{G}_{l_1 l_2 l_3}^{m_1 m_2 m_3} = \sqrt{\frac{(2l_1+1)(2l_2+1)(2l_3+1)}{4\pi}} \begin{pmatrix} l_1 & l_2 & l_3 \\ 0 & 0 & 0 \end{pmatrix} \begin{pmatrix} l_1 & l_2 & l_3 \\ m_1 & m_2 & m_3 \end{pmatrix}. \quad (\text{A.9})$$

Now let us consider the non-Gaussian perturbations given in (2.1)-(2.2). As is shown in (2.23), the bispectrum of these Gaussian-squared type perturbations can be approximated in the form of the local-type bispectrum,

$$B^{X_1 X_2 X_3}(k_1, k_2, k_3) \simeq 8A\gamma_{X_1}\gamma_{X_2}\gamma_{X_3}\mathcal{P}_g(k_0) [P_g(k_1)P_g(k_2) + (2 \text{ cyclic perms})], \quad (\text{A.10})$$

where the factor γ_X should be γ_1 for $X = \mathcal{R}$ and γ_2 for $X = \mathcal{S}$. Here, the factor $A \simeq [(k/k_0)^{n_g-1}]_{L^{-1}}^{k_{\max}} / (n_g - 1)$ depends on wave numbers weakly, and the scale dependence of A can be safely neglected as long as CMB anisotropies (i.e. T and E) are concerned. In the following analysis, we simply replace A with unity. Then the reduced bispectrum in (A.6) can be rewritten as

$$b_{l_1 l_2 l_3}^{P_1 P_2 P_3} = \sum_{X_1 X_2 X_3} 8\gamma_{X_1}\gamma_{X_2}\gamma_{X_3}\mathcal{P}_g(k_0) [b_{l_1 l_2 l_3}^{X_1 P_1, X_2 P_2 X_3 P_3} + (2 \text{ cyclic perms})]. \quad (\text{A.11})$$

Here, $b_{l_1 l_2 l_3}^{X_1 P_1, X_2 P_2 X_3 P_3}$ is given as

$$b_{l_1 l_2 l_3}^{X_1 P_1, X_2 P_2 X_3 P_3} \equiv \int r^2 dr \alpha_l^{X_1 P_1}(r) \beta_l^{X_2 P_2}(r) \beta_l^{X_3 P_3}(r), \quad (\text{A.12})$$

with $\alpha_l^{XP}(r)$ and $\beta_l^{XP}(r)$ being defined as

$$\alpha_l^{XP}(r) \equiv \frac{2}{\pi} \int k^2 dk g_l^{XP}(k) j_l(kr), \quad (\text{A.13})$$

$$\beta_l^{XP}(r) \equiv \frac{2}{\pi} \int k^2 dk P_g(k) g_l^{XP}(k) j_l(kr). \quad (\text{A.14})$$

For later convenience, we define the following set of non-linearity parameters

$$f_{\text{NL}}^{(1)} = 8\gamma_1^3 \mathcal{P}_g(k_0), \quad (\text{A.15})$$

$$f_{\text{NL}}^{(2)} = 8\gamma_1^2 \gamma_2 \mathcal{P}_g(k_0), \quad (\text{A.16})$$

$$f_{\text{NL}}^{(3)} = 8\gamma_1 \gamma_2^2 \mathcal{P}_g(k_0), \quad (\text{A.17})$$

$$f_{\text{NL}}^{(4)} = 8\gamma_2^3 \mathcal{P}_g(k_0). \quad (\text{A.18})$$

Then the reduced bispectrum can be given as

$$b_{l_1 l_2 l_3}^{P_1 P_2 P_3} = \sum_{j=1}^4 f_{\text{NL}}^{(j)} b_{l_1 l_2 l_3}^{P_1 P_2 P_3(j)}, \quad (\text{A.19})$$

where $\{b_{l_1 l_2 l_3}^{P_1 P_2 P_3(j)}\}$ are template bispectra for the nonlinearity parameters $f_{\text{NL}}^{(j)}$, which are defined as

$$b_{l_1 l_2 l_3}^{P_1 P_2 P_3(1)} = b_{l_1 l_2 l_3}^{\mathcal{R}P_1, \mathcal{R}P_2 \mathcal{R}P_3} + (2 \text{ cyclic perms}), \quad (\text{A.20})$$

$$b_{l_1 l_2 l_3}^{P_1 P_2 P_3(2)} = [b_{l_1 l_2 l_3}^{SP_1, \mathcal{R}P_2 \mathcal{R}P_3} + b_{l_1 l_2 l_3}^{\mathcal{R}P_1, SP_2 \mathcal{R}P_3} + b_{l_1 l_2 l_3}^{\mathcal{R}P_1, \mathcal{R}P_2 SP_3}] + (2 \text{ cyclic perms}), \quad (\text{A.21})$$

$$b_{l_1 l_2 l_3}^{P_1 P_2 P_3(3)} = [b_{l_1 l_2 l_3}^{\mathcal{R}P_1, SP_2 SP_3} + b_{l_1 l_2 l_3}^{SP_1, \mathcal{R}P_2 SP_3} + b_{l_1 l_2 l_3}^{SP_1, SP_2 \mathcal{R}P_3}] + (2 \text{ cyclic perms}), \quad (\text{A.22})$$

$$b_{l_1 l_2 l_3}^{P_1 P_2 P_3(4)} = b_{l_1 l_2 l_3}^{SP_1, SP_2 SP_3} + (2 \text{ cyclic perms}). \quad (\text{A.23})$$

Now let us move on to the Fisher matrix analysis. According to Refs. [49, 50], given template bispectra $b_{l_1 l_2 l_3}^{P_1 P_2 P_3(j)}$, the Fisher matrix for the nonlinearity parameters $f_{\text{NL}}^{(j)}$ can be approximately given as

$$F_{jj'} = f_{\text{sky}} \sum_{l_1 \leq l_2 \leq l_3} \frac{(2l_1 + 1)(2l_2 + 1)(2l_3 + 1)}{4\pi} \begin{pmatrix} l_1 & l_2 & l_3 \\ 0 & 0 & 0 \end{pmatrix}^2 \quad (\text{A.24})$$

$$\times \sum_{P_1 P_2 P_3} \sum_{P'_1 P'_2 P'_3} b_{l_1 l_2 l_3}^{P_1 P_2 P_3(j)} [\mathbf{Cov}_{l_1 l_2 l_3}^{-1}]^{P_1 P_2 P_3 | P'_1 P'_2 P'_3} b_{l_1 l_2 l_3}^{P'_1 P'_2 P'_3(j')}, \quad (\text{A.25})$$

where f_{sky} is the fraction of the sky covered by observations and $[\mathbf{Cov}_{l_1 l_2 l_3}^{-1}]^{P_1 P_2 P_3 | P'_1 P'_2 P'_3}$ is the inverse of covariance matrix. The covariance matrix $[\mathbf{Cov}_{l_1 l_2 l_3}]^{P_1 P_2 P_3 | P'_1 P'_2 P'_3}$ should be given in the limit of weak non-Gaussianity as

$$[\mathbf{Cov}_{l_1 l_2 l_3}]^{P_1 P_2 P_3 | P'_1 P'_2 P'_3} = \Delta_{l_1 l_2 l_3} \mathcal{C}_{l_1}^{P_1 P'_1} \mathcal{C}_{l_2}^{P_2 P'_2} \mathcal{C}_{l_3}^{P_3 P'_3}, \quad (\text{A.26})$$

where $\mathcal{C}_l^{PP'} = C_l^{PP'} + N_l^{PP'}$ is the sum of signal ($C_l^{PP'}$) and noise ($N_l^{PP'}$) power spectra, and $\Delta_{l_1 l_2 l_3}$ takes values 6, 2, 1 for the cases that all l 's are the same, only two of them are the same and otherwise, respectively. For the noise power spectrum, we adopt the Knox's formula [51],

$$N_l^{PP'} = \delta_{PP'} \theta_{\text{FWHM}}^2 \sigma_P^2 \exp \left[l(l+1) \frac{\theta_{\text{FWHM}}^2}{8 \ln 2} \right], \quad (\text{A.27})$$

where θ_{FWHM} is the full width at half maximum of the Gaussian beam, and σ_P is the root mean square of the instrumental noise per pixel. For cases of multi-frequency observations, $N_l^{PP'}$ is given via quadrature sum over frequency channels. In Table 1, we summarized the survey parameters for Planck that we adopt in what follows. In addition, we set the sky coverage f_{sky} to 0.7.

To translate the forecasted constraints on $f_{\text{NL}}^{(j)}$ from the Fisher matrix into those on γ_1 , γ_2 and $\mathcal{P}_g(k_0)$, we define an effective $\Delta\chi^2$ as follows

$$\Delta\chi^2 \equiv \sum_{jj'} f_{\text{NL}}^{(j)} F_{jj'} f_{\text{NL}}^{(j')}. \quad (\text{A.28})$$

The expected allowed regions in the γ_1 and γ_2 plane are shown in Fig. 6. Note that $\mathcal{P}_g(k_0)$ is degenerate with γ_1 and γ_2 , and we can constrain only the combinations $\gamma_1 \mathcal{P}_g(k_0)$ and $\gamma_2 \mathcal{P}_g(k_0)$. As can be read from the figure, when $\gamma_1 = 0$ and $\gamma_2 = 1$, $\mathcal{P}_g(k_0) = 10^{-5}$ would be marginally allowed at 2σ level by Planck for $1.5 \lesssim n_g \lesssim 2$.

bands [GHz]	θ_{FWHM} [arcmin]	σ_T [μK]	σ_P [μK]
30	33.0	2.0	2.8
44	24.0	2.7	3.9
70	14.0	4.7	6.7
100	10.0	2.5	4.0
143	7.1	2.2	4.2
217	5.0	4.8	9.8
353	5.0	14.7	29.8

Table 1. Survey parameters adopted in our analysis for Planck. We here assume 1-year duration of observation.

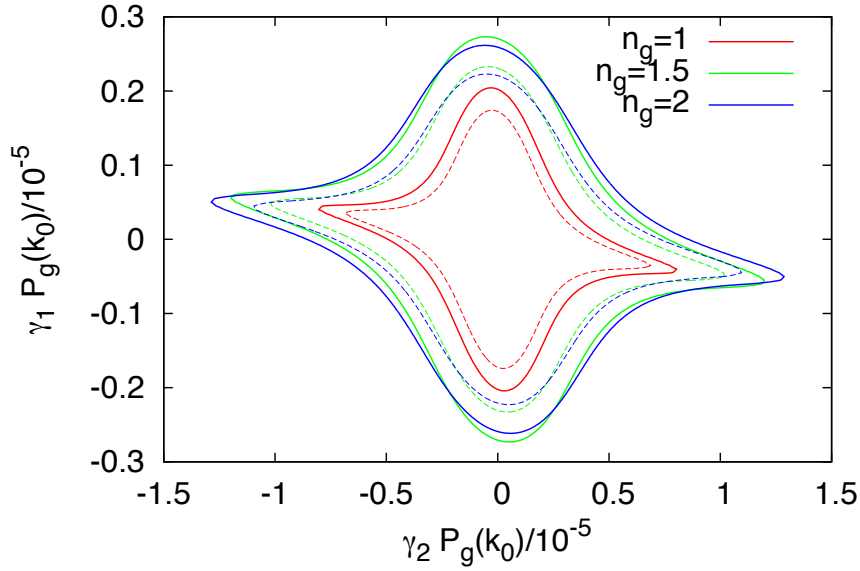


Figure 6. Forecasted constraints on γ_1 and γ_2 in cases of $n_g = 1$ (red), 1.5 (green) and 2 (blue) are shown. Thick solid and thin dashed lines correspond to constraints at 1 and 2 σ levels, respectively.

In addition, we can also compute the expected constraint on $f_{\text{NL}}^{\text{loc},\nu}$ from Planck by performing the Fisher matrix analysis in the similar manner. Given the primordial bispectrum of (4.14), the template bispectrum $\tilde{b}_{l_1 l_2 l_3}^{P_1 P_2 P_3, \nu}$ of the non-linearity parameter $f_{\text{NL}}^{\text{loc},\nu}$ should be given as

$$\tilde{b}_{l_1 l_2 l_3}^{P_1 P_2 P_3, \nu} = -\frac{6}{5} \int r^2 dr \tilde{\alpha}_{l_1}^{P_1}(r) \tilde{\beta}_{l_2}^{P_2}(r) \tilde{\beta}_{l_3}^{P_3}(r), \quad (\text{A.29})$$

with $\tilde{\alpha}_l^P(r)$ and $\tilde{\beta}_l^P(r)$ being defined as

$$\tilde{\alpha}_l^P(r) \equiv \alpha_l^{SP}(r), \quad (\text{A.30})$$

$$\tilde{\beta}_l^P(r) \equiv \frac{2}{\pi} \int k^2 dk P_S(k) g_l^{SP}(k) j_l(kr). \quad (\text{A.31})$$

The reduced bispectrum is given by $b_{l_1 l_2 l_3}^{P_1 P_2 P_3, \nu} = f_{\text{NL}}^{\text{loc}, \nu} \tilde{b}_{l_1 l_2 l_3}^{P_1 P_2 P_3, \nu}$. When P_S is scale-invariant, using the Planck survey parameters given in Table 1, we find the 1σ error on $f_{\text{NL}}^{\text{loc}, \nu} \beta_{\text{iso}}^2$ is expected to be 41. Thus, if β_{iso} is assumed to be 10^{-1} , $f_{\text{NL}}^{\text{loc}, \nu}$ can be as large as 10^4 at around 2σ level.

References

- [1] A. A. Starobinsky, Phys. Lett. B **91**, 99 (1980). A. H. Guth, Phys. Rev. D **23**, 347 (1981); K. Sato, Mon. Not. Roy. Astron. Soc. **195**, 467 (1981).
- [2] J. M. Maldacena, JHEP **0305**, 013 (2003) [astro-ph/0210603].
- [3] P. A. R. Ade *et al.* [Planck Collaboration], arXiv:1303.5082 [astro-ph.CO].
- [4] Burigana, C., de Zotti, G., & Danese, L. 1995, A&A, 303, 323
- [5] R. Khatri and R. A. Sunyaev, JCAP **1209**, 016 (2012) [arXiv:1207.6654 [astro-ph.CO]].
- [6] Y. B. Zeldovich and R. A. Sunyaev, Astrophys. Space Sci. **4**, 301 (1969).
- [7] R. A. Sunyaev and Y. B. Zeldovich Astrophys. Space Sci. **7**, 20 (1970).
- [8] Danese, L.; de Zotti, G. : *Double Compton process and the spectrum of the microwave background*, Astronomy and Astrophysics, vol. 107, no. 1, Mar. 1982, p. 39-42. Research supported by the Consiglio Nazionale delle Ricerche.
- [9] C. Burigana, L. Danese, and G. de Zotti, Astron. Astrophysics, **246**, 49 (1991)
- [10] W. Hu, D. Scott and J. Silk, Astrophys. J. **430**, L5 (1994) [astro-ph/9402045].
- [11] J. Chluba, S. Y. Sazonov and R. A. Sunyaev, [astro-ph/0611172].
- [12] R. Khatri and R. A. Sunyaev, JCAP **1206**, 038 (2012) [arXiv:1203.2601 [astro-ph.CO]].
- [13] R. A. Sunyaev and Y. B. Zeldovich, Astrophys. Space Sci. **9**, 368 (1970).
- [14] J. D. Barrow & P. Coles, Mon. Not. Roy. Astron. Soc., **248**, 52 (1991).
- [15] R. A. Daly, Astrophys. J. **371**, 14 (1991).
- [16] A. Ota, T. Takahashi, H. Tashiro and M. Yamaguchi, arXiv:1406.0451 [astro-ph.CO].
- [17] J. Chluba, L. Dai, D. Grin, M. Amin and M. Kamionkowski, arXiv:1407.3653 [astro-ph.CO].
- [18] J. C. Mather, E. S. Cheng, D. A. Cottingham, R. E. Eplee, D. J. Fixsen, T. Hewagama, R. B. Isaacman and K. A. Jesnsen *et al.*, Astrophys. J. **420**, 439 (1994).
- [19] D. J. Fixsen, E. S. Cheng, J. M. Gales, J. C. Mather, R. A. Shafer and E. L. Wright, Astrophys. J. **473**, 576 (1996) [astro-ph/9605054].
- [20] R. Salvaterra and C. Burigana, Mon. Not. Roy. Astron. Soc. **336**, 592 (2002) [astro-ph/0203294].
- [21] A. Kogut, D. J. Fixsen, D. T. Chuss, J. Dotson, E. Dwek, M. Halpern, G. F. Hinshaw and S. M. Meyer *et al.*, JCAP **1107**, 025 (2011) [arXiv:1105.2044 [astro-ph.CO]].
- [22] P. Andre *et al.* [PRISM Collaboration], JCAP **1402**, 006 (2014) [arXiv:1306.2259 [astro-ph.CO]].
- [23] E. Pajer and M. Zaldarriaga, Phys. Rev. Lett. **109**, 021302 (2012) [arXiv:1201.5375 [astro-ph.CO]].
- [24] J. Ganc and E. Komatsu, Phys. Rev. D **86**, 023518 (2012) [arXiv:1204.4241 [astro-ph.CO]].
- [25] J. B. Dent, D. A. Easson and H. Tashiro, Phys. Rev. D **86**, 023514 (2012) [arXiv:1202.6066 [astro-ph.CO]].

- [26] J. Chluba and D. Grin, Mon. Not. Roy. Astron. Soc. **434**, 1619 (2013) [arXiv:1304.4596 [astro-ph.CO]].
- [27] R. Khatri, R. A. Sunyaev and J. Chluba, Astron. Astrophys. **543**, A136 (2012) [arXiv:1205.2871 [astro-ph.CO]].
- [28] Gould, R. J.: *The cross section for double Compton scattering*, Astrophysical Journal, Part 1 (ISSN 0004-637X), vol. 285, Oct. 1, 1984, p. 275-278.
- [29] W. Hu and J. Silk, Phys. Rev. D **48**, 485 (1993).
- [30] C. -P. Ma and E. Bertschinger, Astrophys. J. **455**, 7 (1995) [astro-ph/9506072].
- [31] J. Chluba, R. Khatri and R. A. Sunyaev, Mon. Not. Roy. Astron. Soc. **425**, 1129 (2012) [arXiv:1202.0057 [astro-ph.CO]].
- [32] D. H. Lyth, C. Ungarelli and D. Wands, Phys. Rev. D **67**, 023503 (2003) [astro-ph/0208055].
- [33] M. Kawasaki, K. Miyamoto, K. Nakayama and T. Sekiguchi, JCAP **1202**, 022 (2012) [arXiv:1107.4962 [astro-ph.CO]].
- [34] T. Kobayashi, F. Takahashi, T. Takahashi and M. Yamaguchi, JCAP **1203**, 036 (2012) [arXiv:1111.1336 [astro-ph.CO]].
- [35] E. Kawakami, M. Kawasaki, K. Miyamoto, K. Nakayama and T. Sekiguchi, JCAP **1207**, 037 (2012) [arXiv:1202.4890 [astro-ph.CO]].
- [36] I. Affleck and M. Dine, Nucl. Phys. B **249**, 361 (1985).
- [37] M. Kawasaki, F. Takahashi and M. Yamaguchi, Phys. Rev. D **66**, 043516 (2002) [hep-ph/0205101].
- [38] A. D. Linde and V. F. Mukhanov, Phys. Rev. D **56**, 535 (1997) [astro-ph/9610219].
- [39] L. Boubekeur and D. H. Lyth, Phys. Rev. D **73**, 021301 (2006) [astro-ph/0504046].
- [40] T. Suyama and F. Takahashi, JCAP **0809**, 007 (2008) [arXiv:0804.0425 [astro-ph]].
- [41] M. Bucher, K. Moodley and N. Turok, Phys. Rev. D **62**, 083508 (2000) [astro-ph/9904231].
- [42] S. Dodelson, Amsterdam, Netherlands: Academic Pr. (2003) 440 p
- [43] E. Pajer and M. Zaldarriaga, JCAP **1302**, 036 (2013) [arXiv:1206.4479 [astro-ph.CO]].
- [44] D. Blas, J. Lesgourgues and T. Tram, JCAP **1107**, 034 (2011) [arXiv:1104.2933 [astro-ph.CO]].
- [45] D. Langlois and B. van Tent, Class. Quant. Grav. **28**, 222001 (2011) [arXiv:1104.2567 [astro-ph.CO]].
- [46] D. Langlois and B. van Tent, JCAP **1207**, 040 (2012) [arXiv:1204.5042 [astro-ph.CO]].
- [47] C. Hikage, M. Kawasaki, T. Sekiguchi and T. Takahashi, JCAP **1303**, 020 (2013) [arXiv:1212.6001 [astro-ph.CO]].
- [48] A. Lewis, A. Challinor and A. Lasenby, Astrophys. J. **538**, 473 (2000) [astro-ph/9911177].
- [49] E. Komatsu and D. N. Spergel, Phys. Rev. D **63**, 063002 (2001) [arXiv:astro-ph/0005036].
- [50] D. Babich and M. Zaldarriaga, Phys. Rev. D **70**, 083005 (2004) [arXiv:astro-ph/0408455].
- [51] L. Knox, Phys. Rev. D **52**, 4307 (1995) [arXiv:astro-ph/9504054].